Draft version May 3, 2024
Typeset using LaTeX default style in AASTeX631

Verification of Theoretical Period-Luminosity Equations via Photometric Analysis of Variable Stars OP Puppis, X Ari, and RU Scl

Jacob F. Hansman,[1] Gina Pantano,[2] and Dr. Michael Fitzgerald[3]

[1] *University of Tampa, Department of Physics and Astronomy, 401 W. Kennedy Blvd, Tampa, FL 33606, USA*
[2] *University of South Florida, Department of Physics, 4202 E Fowler Ave, Tampa, FL 33620, USA*
[3] *Las Cumbres Observatory, Eltham, Victoria, Australia*

ABSTRACT

Photometric analysis via the python pipeline *astrosource* was performed on 3 variable stars; OP Puppis, X Ari, and RU Scl from the cadenced imaging of the OSS observatory network in order to verify the theoretical period-luminosity equations proposed by Catelan et. al. in 2004 and in 2008. We found luminosity pulsation periods of 2.597 days, 0.652 days, and 0.494 days for OP Puppis, X Ari, and RU Scl respectively. Average distances were found for OP Puppis, X Ari, and RU Scl across the Bessell V (5448 Å) and SDSS ip (8700 Å) filters of (2737.5 ± 26)pc, (565 ± 24.5)pc, and (780.5 ± 34)pc respectively. Results indicate that the period-luminosity equation evaluated for the PanSTARRS Z (7545 Å) filter proved inadequate when comparing resultant distances against GAIA DR3 geometric parallax measurements, but the equations for the Bessel V and SDSS ip filter produce results consistent with those of GAIA with average differences at 3.8% and 2.2%.

1. INTRODUCTION

The importance of variable stars within astronomy has been well known for decades, as they are known as one of the "standard candles" of our universe, aiding in distance determination through known relationships that arise through the periodicity of their luminosity pulsation. Many different standard candles, including different types of variable stars, the Tip of the Red Giant Branch stars, and type Ia Supernovae all contribute to the creation of an extragalactic distance ladder. This ladder of distance determination begins with geometric parallax measurements of nearby stars within our galaxy, and reaches out further in distance beyond our galaxy with multiple different distance determination methodologies that aim to both calibrate the previous step in the ladder and ensure minimal uncertainty in the method's own calculations. A well calibrated distance ladder allows for the determination of the Hubble Constant, H_0, that provides the measured expansion rate of our universe. Currently within the field, there is a 5σ difference between the H_0 value found from a well calibrated extragalactic distance ladder, such as the SH0Es survey ladder Breuval et al. (2024), and the H_0 value found from examination of the Cosmic Microwave Background through the lens of the ΛCDM model of the universe. This indicates the potential for discovery of either new Physics or a re-write of the current state of the field of Cosmology in the near future. This study, along with around 200 other similar studies, aims to contribute toward calibration of the first rung of the distance ladder, to verify the accuracy of RR Lyrae Period-Luminosity (PL) relationships, proposed by Catelan et. al. in 2004 and in 2008, against the DR3 parallax measurements from ESA's GAIA mission, all in support of the search for answers among the current "Cosmological Crisis".

Analysis was performed on three variable stars, OP Puppis (OP Pup), X Ari, and RU Scl for the verification of the RR Lyrae (RRL) PL equations within this study. OP Pup's properties, including its prolonged luminosity pulsation period and high mass, classify it as a type II BL Herculis Cepheid Ripepi et al. (2021), but it was previously recognized as an RR Lyrae type star prior to a Harvard observational study in 1996 where a much longer period than expected was found Williams (1996). While both type II Cepheids (T2Cs) and RR Lyrae stars are utilized as distance indicators, with T2Cs being even more visible in high extinction environments as they are one to five mag brighter than RRLs, the

Corresponding author: Jacob F. Hansman
jacob.hansman@spartans.ut.edu

distinction between the types of variable stars is important in that T2Cs period-luminosity relations are not commonly known to be affected by metallicity in the optical and near to mid-IR wavelengths. RR Lyrae stars are another subclass of variable stars that are low-mass and exhibit periods of typically only .2 to 1 day. The two other investigated stars, X Ari and RU Scl, are RR Lyrae stars of subclass RRab. RR Lyrae stars are characterised by a few different subclasses, called Bailey types. Bailey types are distinguished by the type of pulsation they exhibit, specifically the overtone exhibited in the yielded light curve associated with a star's luminosity pulsation. RRab type RRLs are classified as fundamental tone pulsators, placed in this classification because they exhibit light curves with high amplitudes and longer periods. RRc type RRLs are classified as first-overtone pulsators, exhibiting light curves that have a higher frequency, lower amplitudes, and a more symmetric, sinusoidal pattern. This first-overtone pulsation is still caused by the burning of He within the core of the star, but there lies a "reversal of the phase of luminosity variation at the pulsation node, deep in the star" that causes the shortening of the period and lowering of the amplitude Stellingwerf et al. (1987). There also exists a subclass RRd where a star exhibits the properties of both RRab and RRc stars, as well as subclass type "e" stars, or second-overtone pulsators. Both RRLs and T2Cs are typically associated with old stellar populations due to the physical explanation for their pulsation; that being the burning of He within their cores. This process only occurs, depending on the star's mass, after around 10 Gyr. However, T2Cs, due to their far higher luminosity on average than RRLs, are able to be seen in external galaxies whereas viewing of RRLs is only detectable in old stellar populations. Catelan et al. in 2004 and 2008 were able to develop theoretical relationships relating the periodicity, metallicity, and absolute magnitude of a given RR Lyrae star for observations using some different widespread use filters; Bessell B, Bessell V, SDSS ip, and PanSTARRS z.

Computer-assisted photometric analysis studies of RR Lyrae variable stars have been carried out for decades. The first study that demonstrated work similar to this study dates back to 1965, where Lafler and Kinman performed photometric analysis on an IBM 1620 Lafler & Kinman (1965). Ongoing research is being performed with massive improvements since 1965 to both observational and computational technology to verify whether these theoretical relationships put forth by Catelan et. al. in 2004 and in 2008 yield distance measurements that are in agreement with the distances yielded from the increasingly precise parallax measurements of stellar surveys such as GAIA Lindegren et al. (2021), and this study aims to support this ongoing effort. Recent studies, such as Marconi et al. (2015), aim to put forth newly derived PL equations similar to the equations utilized in this study for further analysis carried out in a manner similar to the one taken on by this study.

While it is thought to be known that metallicity has little effect on the period-luminosity relationship for type II Cepheids, so therefore it is unlikely to have cross-compatibility between RRL and T2C PL equations; it is also known that T2Cs are useful in numerous other ways such as their greater visibility in higher extinction environments and their general PL relation similarity to RRL PL relation in the near-infrared. For these reasons, the analysis of OP Pup was included in this study alongside the study of the two RRab RRLs, X Ari and RU Scl.

2. MATERIALS & METHODS

2.1. *Observations*

This study utilized images collected from the Las Cumbres Observatory, an observatory based out of Santa Barbara, California that operates a network of a total of 25 telescopes located at seven different sites around the world. Of these seven sites, our specific study gathered data as both 1 image test observations and 2 to 3 week extended cadence observations from telescopes located at the Siding Spring Observatory, the Haleakala Observatory, and the Teide Observatory. The Siding Spring Observatory is located in New South Wales, Australia at an elevation of 1116 meters. It has one 2 meter telescope, two 1 meter telescopes, and two .4 meter telescopes. These telescopes at Siding Spring were specifically utilized to take the images for the second and third round of test images for RU Scl, the first round of test images for X Ari, and a portion of the cadence observation images for X Ari. The Haleakala Observatory is located in Maui, Hawii at an elevation of 3055 meters. It holds one 2 meter telescope and two .4 meter telescopes. These telescopes at Haleakala were specifically utilized for the first round of test images for RU Scl. The Teide Observatory is located at Tenerife, Canary Islands, Spain at an elevation of 2330 meters. It has two .4 meter telescopes and two 1 meter telescopes. These telescopes at Teide were specifcally utilized for a portion of X Ari's extended cadence observation.

2.2. *Calculations & Image Photometry*

Rounds of test images for each of the 3 stars were taken in order to determine the proper exposure times to use for the extended cadence observations of each star. For all the images and data collected, four filters were utilized; Bessell-B at 4361 Å, Bessell-V at 5448 Å, PanSTARRS-Z at 7545 Å, and SDSS-ip at 8700 Å. To properly calculate the exposure times needed for each of the three stars' cadence observations, these test images were analyzed within an image processing and photometric extraction software called AstroImageJ that allowed for counting the pixels within a certain aperture around the selected star to compare with the background of the sky Collins et al. (2017). The optimal times for the X Ari cadence observation were determined to be 12 seconds in B, V, and i and 30 seconds in Z. Whereas the optimal times for RU Scl's cadence observation were determined to be comparable at 29 seconds in B, 10 seconds in V, 12 seconds in i, and 40 seconds in Z. OP Pup's optimal exposure times for the extended cadence observation were determined to be 54.92 seconds in B, 14.68 seconds in V, 11.5 seconds in i, and 40.5 seconds in Z. After receiving the images back from each of the three cadence observations, they were processed utilizing the OSS Pipeline with an Astropy-based script in python called astrosource that determined the apparent magnitude and as well as the luminosity pulsation period of each of the stars Fitzgerald et al. (2021). This process provided six different photometric methodologies to work with in order to extract the most accurate data from the collected images. These types were APT, SEK, SEA, DAO, DOP, and PSX. Half of these, being APT, SEK, and SEA, are based on the system of aperature photometry like described above within AstroImageJ. The other half of these, being DOP, DAO, and PSX are based on the system of Point Spread Function photometry (PSF). In addition to this data from the cadence observation images processed through astrosource, reported values for $[Fe/H]$ of each of the stars within academic literature were utilized in conjunction with the proposed theoretical PL relationships from Catelan et al. (2004), Cáceres & Catelan (2008) to produce a value for the absolute magnitude of each star,

$$M_V = 2.288 + 0.882 \log Z + 0.108 (\log Z)^2 \tag{1}$$

$$M_z = 0.839 - 1.295 \log P + 0.211 \log Z \tag{2}$$

$$M_i = 0.908 - 1.035 \log P + 0.220 \log Z \tag{3}$$

And to gather a value for Log Z:

$$\log Z = [M/H] - 1.765 \tag{4}$$

$$[M/H] = [Fe/H] + \log (0.638 f + 0.362), (f = 10^{0.3}) \tag{5}$$

Using the B-V value and maximum estimated extinction value from the NASA/IPAC Infrared Science Archive, the absolute magnitude, apparent magnitude, and extinction value were used within the distance modulus,

$$d = 10^{((m-M-A+5)/5)} \tag{6}$$

which allowed for the determination of the distances to X Ari and RU Scl. The process for OP Pup varied slightly, as it is recognized as a type II Cepheid rather than an RR Lyrae, so 2 different sets of period-luminosity equations given by Carroll & Ostlie (1996) and Sandage et al. (2009)

$$M_V = -2.81 \log P - 1.43 \tag{7}$$

And

$$M_V = -(2.588 \pm 0.045) \log P - (1.400 \pm 0.035) \tag{8}$$

$$M_B = -(2.222 \pm 0.054) \log P - (1.182 \pm 0.041) \tag{9}$$

$$M_I = -(2.862 \pm 0.035) \log P - (1.847 \pm 0.027) \tag{10}$$

were utilized to gather the absolute magnitude of OP Pup instead of the newly proposed equations in order to improve accuracy and stay consistent with the current understanding of Cepheid behavior. From there on out the process was similar as the distance modulus was used to gather a distance measurement comparable to GAIA's parallax measurements.

3. RESULTS

OP Puppis								
Type	**ICRS Coordinates [RA, Dec]**	**Reported Period**	T_{eff}	$[Fe/H]$	**Log(g)**	**Reported Distance (pc)**	**Reported Dist. Method**	**References**
DCEP	N/A	2.598824	6030	-0.11	1.4	N/A	N/A	(Ripepi V. et al., 2021)
DCEP	N/A	N/A	6200	-0.11	1.8	N/A	N/A	(Ripepi V. et al., 2021)
DCEP	N/A	N/A	6230	-0.11	1.6	N/A	N/A	(Ripepi V. et al., 2021)
DCEP	[07 39 21.49, -17 20 49.1]	2.598777	N/A	N/A	N/A	N/A	N/A	(GAIA et al., 2022)
						4226.543	parallax	(GAIA et al., 2020)
						2508.9597	parallax	(GAIA et al., 2023)

Table 1. The table above displays gathered information from previous studies regarding the type II Cepheid variable star OP Puppis.

RU Scl								
Type	**ICRS Coordinates [RA, Dec]**	**Reported Period**	T_{eff}	$[Fe/H]$	**Log(g)**	**Reported Dist. Method**	**Reported Distance**	**References**
RRab	[00 02 48.11, -25 56 43.1]	.493352	N/A	N/A	N/A	parallax	798.148	(GAIA et al., 2022)
	N/A	N/A	6005	N/A	N/A	ST-L	928.883	(Steinmetz M. et al., 2020)
	N/A	N/A	7250	N/A	N/A	ST-L	891.420	(Steinmetz M. et al., 2020)
	N/A	N/A	6150	N/A	N/A	N/A	N/A	(Crestani J. et al., 2021)
RRab	[00 02 48.11, -25 56 43.1]	.493358	N/A	N/A	N/A	N/A	N/A	(GAIA et al., 2018)
	N/A	.493000	N/A	-1.27	N/A	N/A	N/A	(Nagarajan P. , Weiszel D. R., and El-Badry K., 2022)

Table 2. The table above displays gathered information from previous studies regarding the RRab RR Lyrae variable star RU Scl.

X Ari									
Type	**ICRS Coordinates [RA, Dec]**	**Reported Period**	T_{eff}	$[Fe/H]$	M_V	**Log(g)**	**Reported Distance (pc)**	**Reported Dist. Method**	**References**
RRab	[03 08 30.88, 10 26 45.2]	.651169	N/A	N/A	N/A	N/A	544.722	parallax	(GAIA et al., 2022)
	N/A	N/A	5898	-2.69	N/A	1.35	N/A	N/A	(Limberg G. et al., 2021)
RRab	N/A	.651	N/A	-2.43	9.5620	N/A	N/A	N/A	(Nagarajan P. , Weiszel D. R., and El-Badry K., 2022)
	N/A	N/A	6109	-2.50	N/A	2.60	N/A	N/A	(Duflot M., Figon P. and Meyssonnier N., 1995)
	N/A	N/A	6109	-2.50	N/A	2.6	N/A	N/A	(Clementini et al., 1995)

Table 3. The table above displays gathered information regarding previous investigations into the RRab RR Lyrae variable star X Ari.

OP Puppis	**B**	**V**	**ip**	**Z**
SEK				
Comparison Catalogue	APASS	APASS	SkyMapper	SkyMapper
Error in calibration	0.01247	0.01158	0.01141	0.01641
Median std. dev. Calibration	0.03945	0.04486	0.04269	0.05918
Max Magnitude	12.12229	11.23029	10.72594	10.57285
Min Magnitude	11.27673	10.62952	10.22278	10.19243
Amplitude	0.84556	0.60077	0.50316	0.38042
Mid Magnitude	11.69951	10.92991	10.47436	10.38264
Dist. Method Period Est. (Days)	2.59800	2.59780	2.60100	2.59820
Dist. Method Period error	0.03450	0.03420	0.03300	0.03240
PDM Method Period Est. (Days)	2.59760	2.59780	2.60140	2.60400
PDM Method Period error	0.03150	0.31500	0.28400	0.02700
Harmonic Anova Method Period Estimate (Days)	2.59830	2.59965	2.59785	2.59965
Lomb-Scargle N=1 Period Estimate (Days)	2.59716	2.59856	2.59776	2.59816
Lomb-Scargle N=2 Period Estimate (Days)	2.59776	2.59916	2.59876	2.59916
PSX				
Comparison Catalogue	APASS	APASS	SkyMapper	PanSTARRS
Error in calibration	0.01464	0.00859	0.00919	0.01573
Median std. dev. Calibration	0.05858	0.03644	0.04695	0.08019
Max Magnitude	12.09831	11.24107	10.58523	10.43928
Min Magnitude	11.38656	10.63824	10.18053	10.28203
Amplitude	0.71175	0.60283	0.40469	0.15724
Mid Magnitude	11.74244	10.93965	10.38288	10.36065
Dist. Method Period Est. (Days)	2.59960	2.57980	2.60280	1.41780
Dist. Method Period error	0.03430	0.19810	0.23860	0.01890
PDM Method Period Est. (Days)	2.59880	2.59840	2.58260	N/A
PDM Method Period error	0.03010	0.16430	0.20250	N/A
Harmonic Anova Method Period Estimate (Days)	2.59785	2.58933	2.54582	1.59524
Lomb-Scargle N=1 Period Estimate (Days)	2.59656	2.61517	2.54675	1.16342
Lomb-Scargle N=2 Period Estimate (Days)	2.59736	2.60136	2.54135	1.01560

Table 4. The above table illustrates the resultant values yielded from the Astrosource analysis of a set of cadenced images of the type II Cepheid variable star OP Puppis.

RU Scl	**B**	**V**	**ip**	**Z**
SEK				
Comparison Catalogue	APASS	APASS	SkyMapper	PanSTARRS
Error in calibration	0.02188	0.01059	0.03833	0.09868
Median std. dev. Calibration	0.03095	0.01059	0.03833	0.13956
Max Magnitude	11.17806	10.67624	10.45315	10.09685
Min Magnitude	9.69551	9.56771	9.66421	9.37014
Amplitude	1.48254	1.10853	0.78893	0.72670
Mid Magnitude	10.43678	10.12197	10.05868	9.73349
Dist. Method Period Est. (Days)	0.49364	0.49364	0.49346	0.49364
Dist. Method Period error	0.00504	0.00493	0.00504	0.00531
PDM Method Period Est. (Days)	0.49364	0.49364	0.49260	0.49364
PDM Method Period error	0.00412	0.00423	0.00407	0.00385
Harmonic Anova Method Period Estimate (Days)	0.49350	0.49340	0.49331	0.49340
Lomb-Scargle N=1 Period Estimate (Days)	0.49307	0.49307	0.49307	0.49311
Lomb-Scargle N=2 Period Estimate (Days)	0.49338	0.49338	0.49334	0.49325
SEA				
Comparison Catalogue	APASS	APASS	SkyMapper	SkyMapper
Error in calibration	0.02888	0.01417	0.01848	0.02451
Median std. dev. Calibration	0.04084	0.01417	0.01848	0.02451
Max Magnitude	11.12217	10.86360	10.65158	10.45653
Min Magnitude	9.71156	9.55369	9.56734	9.73498
Amplitude	1.41061	1.30991	1.08424	0.72155
Mid Magnitude	10.41686	10.20864	10.10946	10.09575
Dist. Method Period Est. (Days)	0.49364	0.49364	0.49364	0.49346
Dist. Method Period error	0.00504	0.00513	0.00508	0.00504
PDM Method Period Est. (Days)	0.49355	0.49355	0.49386	0.49269
PDM Method Period error	0.00398	0.00421	0.00412	0.00392
Harmonic Anova Method Period Estimate (Days)	0.49345	0.49340	0.49340	0.49350
Lomb-Scargle N=1 Period Estimate (Days)	0.49302	0.49302	0.49320	0.49325
Lomb-Scargle N=2 Period Estimate (Days)	0.49334	0.49338	0.49356	0.49335
PSX				
Comparison Catalogue	APASS	APASS	SkyMapper	
Error in calibration	0.04898	0.01729	0.01778	
Median std. dev. Calibration	0.03463	0.02445	0.02514	
Max Magnitude	11.62883	10.81344	10.62031	
Min Magnitude	9.70279	9.50690	9.64749	
Amplitude	1.92604	1.30654	0.97282	
Mid Magnitude	10.66581	10.16017	10.13390	
Dist. Method Period Est. (Days)	0.49368	0.49305	0.49247	
Dist. Method Period error	0.00535	0.00518	0.00554	
PDM Method Period Est. (Days)	0.49422	0.49319	0.49260	
PDM Method Period error	0.00346	0.00394	0.00430	
Harmonic Anova Method Period Estimate (Days)	0.49365	0.49321	0.49306	
Lomb-Scargle N=1 Period Estimate (Days)	0.49338	0.49298	0.49307	
Lomb-Scargle N=2 Period Estimate (Days)	0.49333	0.49338	0.49343	

Table 5. The above table illustrates the resultant values yielded from the Astrosource analysis of a set of cadenced images of the RRab RR Lyrae variable star RU Scl. Data was unable to be produced for the PSX method for the PanSTARRS z filter.

X Ari	**B**	**V**	**ip**	**Z**
SEK				
Comparison Catalogue	APASS	APASS	SDSS	
Error in calibration	0.13905	0.03017	0.04488	
Median std. dev. Calibration	0.27809	0.07390	0.10993	
Max Magnitude	11.45508	9.75896	9.48311	
Min Magnitude	8.80796	8.82607	8.43109	
Amplitude	2.64712	0.93289	1.05202	
Mid Magnitude	10.13152	9.29251	8.95710	
Dist. Method Period Est. (Days)	0.65150	0.65165	0.64930	
Dist. Method Period error	0.00748	0.00985	0.00958	
PDM Method Period Est. (Days)	0.65120	0.65225	0.64975	
PDM Method Period error	0.00555	0.00440	0.00572	
Harmonic Anova Method Period Estimate (Days)	0.32254	0.65191	0.36012	
Lomb-Scargle N=1 Period Estimate (Days)	0.32245	0.65243	0.65209	
Lomb-Scargle N=2 Period Estimate (Days)	0.31965	0.65209	0.65229	
SEA				
Comparison Catalogue	APASS	APASS	APASS	PanSTARRS
Error in calibration	0.02658	0.03213	0.03372	0.06304
Median std. dev. Calibration	0.05944	0.08500	0.05840	0.14097
Max Magnitude	10.22414	9.93894	9.79006	15.58422
Min Magnitude	8.86359	8.80814	8.64255	14.87539
Amplitude	1.36055	1.13080	1.14751	0.70883
Mid Magnitude	9.54386	9.37354	9.72691	15.22980
Dist. Method Period Est. (Days)	0.65165	0.65290	0.65230	0.65165
Dist. Method Period error	0.00600	0.01350	0.00320	0.00538
PDM Method Period Est. (Days)	0.65100	0.65545	0.65335	0.65165
PDM Method Period error	0.00318	0.00390	0.00345	0.00383
Harmonic Anova Method Period Estimate (Days)	0.65164	0.44012	0.40973	0.38403
Lomb-Scargle N=1 Period Estimate (Days)	0.65239	0.65364	0.65484	0.65264
Lomb-Scargle N=2 Period Estimate (Days)	0.65164	0.65304	0.65674	0.65234
PSX				
Comparison Catalogue	APASS	APASS	APASS	
Error in calibration	0.02505	0.02238	0.04314	
Median std. dev. Calibration	0.05011	0.05481	0.09647	
Max Magnitude	10.56784	9.95799	10.76497	
Min Magnitude	8.96064	8.86230	8.62785	
Amplitude	1.60720	1.09569	2.13712	
Mid Magnitude	9.76424	9.41015	9.69641	
Dist. Method Period Est. (Days)	0.65140	0.65290	0.53065	
Dist. Method Period error	0.00365	0.01420	0.00167	
PDM Method Period Est. (Days)	0.65210	0.62865	0.46755	
PDM Method Period error	0.00257	0.00092	0.00005	
Harmonic Anova Method Period Estimate (Days)	0.65200	0.64257	0.36694	
Lomb-Scargle N=1 Period Estimate (Days)	0.65284	0.65344	0.53122	
Lomb-Scargle N=2 Period Estimate (Days)	0.32150	0.65299	0.50797	

Table 6. The above table illustrates the resultant values yielded from the Astrosource analysis of a set of cadenced images of the RRab RR Lyrae variable star X Ari. Data was unable to be produced for both the PSX method and the SEK method for the PanSTARRS z filter.

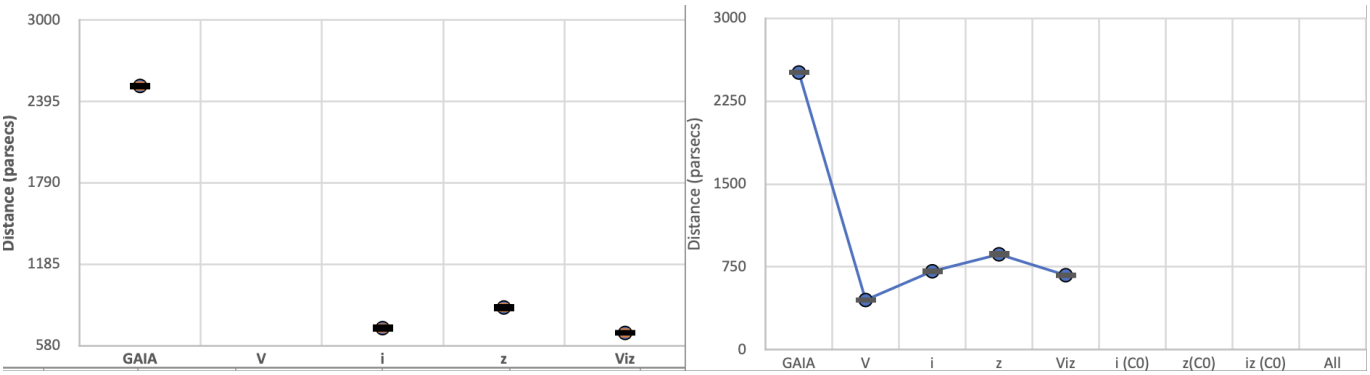

Figure 1. The 2 plots above show the comparison of distance results per filter and against GAIA's parallax measurement in parsecs using the RRL equations (Catelan et al. 2004, 2008) for the type II Cepheid variable star OP Puppis. Through these figures it is clear that the RRL equations are not commutative to other types of variable stars with extended periods.

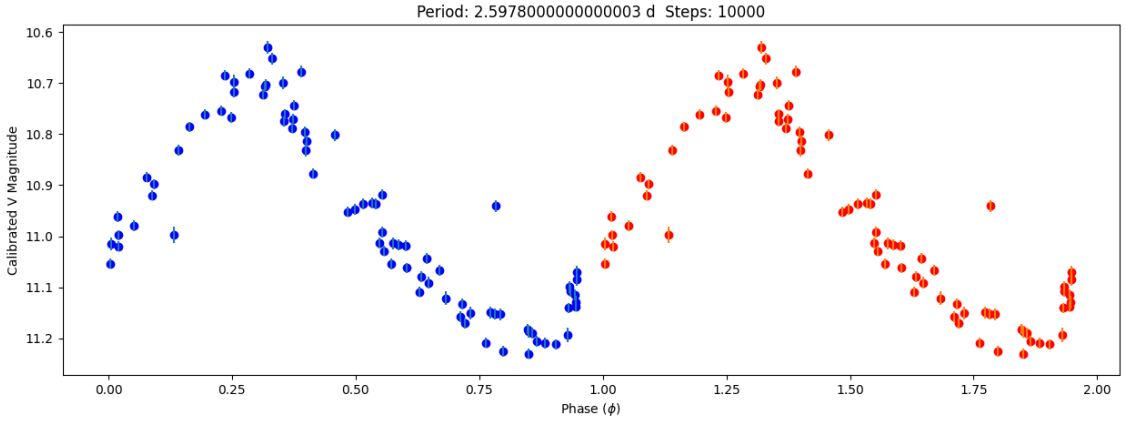

Figure 2. The figure above illustrates the found light curve and resultant period in days for OP Pup in the Bessel V band.

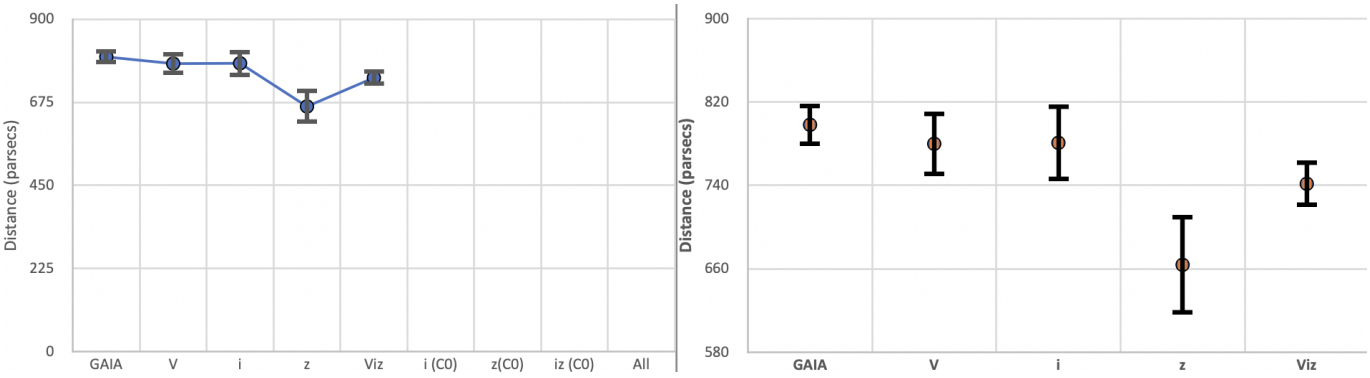

Figure 3. The 2 plots above illustrate the comparison of distance results per filter and against GAIA's parallax measurement in parsecs for RRab type RR Lyrae variable star RU Scl.

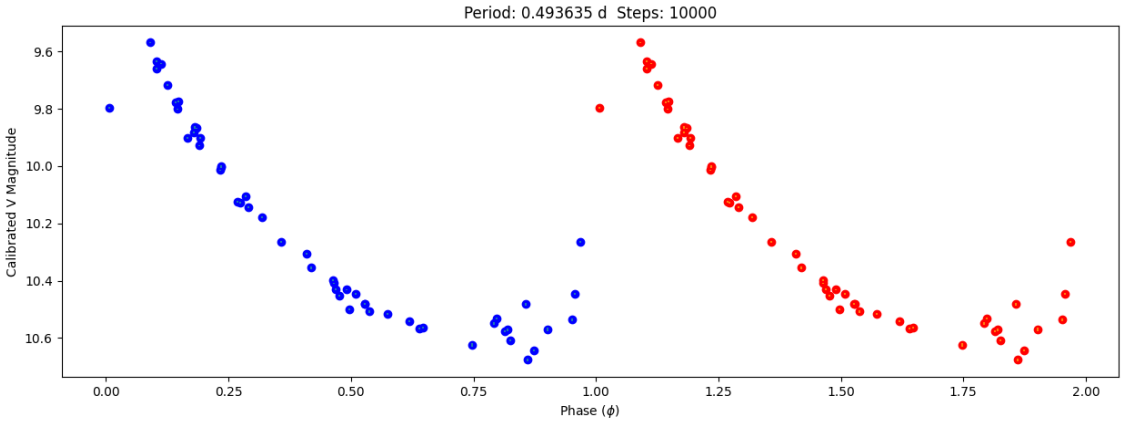

Figure 4. The figure above illustrates the found light curve and resultant period in days for RU Scl in the Bessel V band.

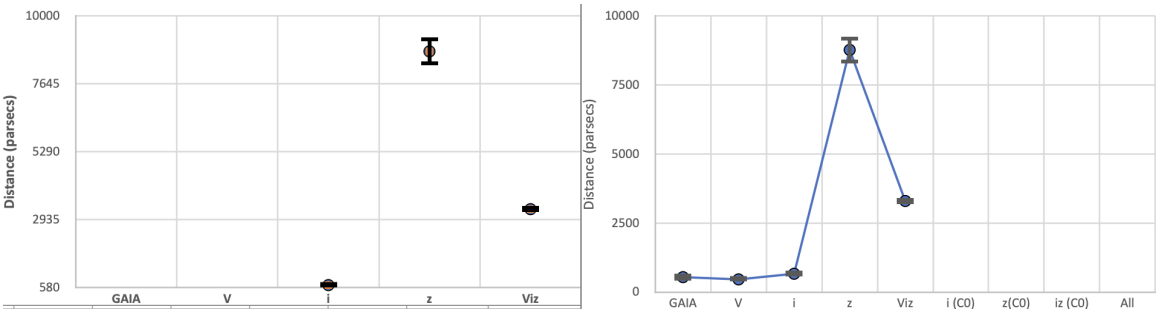

Figure 5. The 2 plots above illustrate the comparison of distance results per filter and against GAIA's parallax measurement in parsecs for RRab type RR Lyrae variable star X Ari. Through these figures it is clear that the data recorded and the calculations performed for images in the Z-filter were inaccurate compared to other filters' data collected.

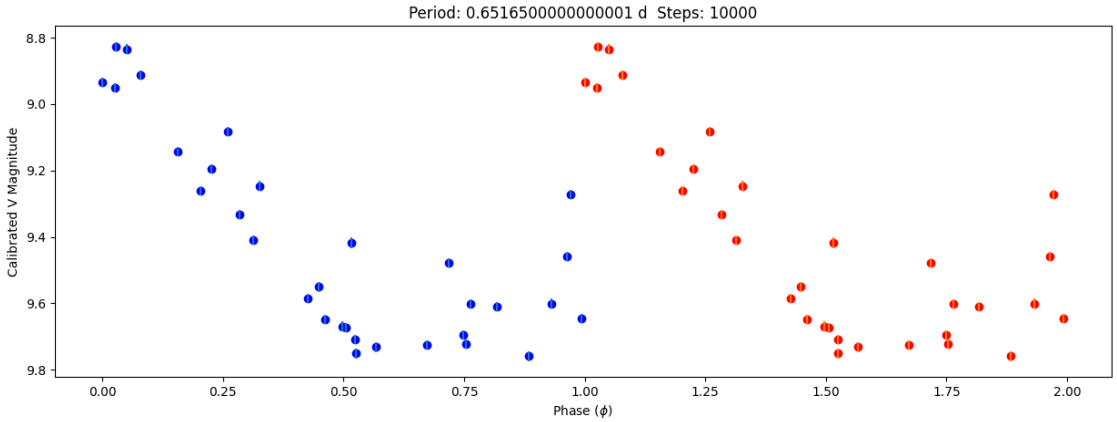

Figure 6. The figure above illustrates the found light curve and resultant period in days for X Ari in the Bessel V band.

OP Puppis (RRL equations)	**B**	**V**	**ip**	**Z**	**GAIA**
Distance (pc)	N/A	450.000	711.000	864.000	2,509.000
Distance error	N/A	25.000	25.000	28.000	23.000
X Ari					
Distance (pc)	N/A	463.000	667.000	8,775.000	544.722
Distance error	N/A	19.000	30.000	483.000	5.578
RU Scl					
Distance (pc)	N/A	780.000	781.000	664.000	798.148
Distance error	N/A	31.000	37.000	48.000	20.194
OP Puppis (DCEP equation 1)					
Distance (pc)	N/A	2,556.670	N/A	N/A	2,509.000
Distance error	N/A	26.000	N/A	N/A	23.000
OP Puppis (DCEP equation 2)					
Distance (pc)	2,398.492	2,416.801	3,058.271	N/A	2,509.000
Distance error	26.000	26.000	26.000	N/A	23.000

Table 7. The table above displays the final resultant yielded distances in parsecs for each star included in this study and the associated errors.

4. DISCUSSION & CONCLUSION

The equations from Carroll & Ostlie (1996), Sandage et al. (2009), and Catelan et al. (2004) and Cáceres & Catelan (2008) described previously for the determination of distance yielded results that were both in agreement and in disagreement with GAIA DR3's parallax distance estimations. The greatest source of error within these distance calculations is generated from the calibration methodology applied by the OSS Pipeline. This calibration method is called the "All-Sky Calibration Pipeline" and it searches through the astrosource created photometry files for each image to identify standard stars within them from a custom standard catalogue of stars from Clem & Landolt (2013) and Clem & Landolt (2016). Also, when possible, the OSS pipeline will match UGRIZ photometry to SDSS and Skymapper catalogues. The selection of these standard star targets uses a standards-picker script that maximizes airmass, color, and number spread for any given time, date, or location at any of the observatories utilized in the OSS network. Once these standards are set and outliers have been rejected, photometric solutions for UBVRI bands are determined by solving for coefficients in the following equations from:

$$U = U_{INST} + Z_U + K_U A + C_U(U-B) + K_{U2}A(U-B) + C_{U2}(U-B)^2 + t_U t \tag{11}$$

$$B = B_{INST} + Z_B + K_B A + C_B(B-V) + K_{B2}A(B-V) + C_{B2}(B-V)^2 + t_B t \tag{12}$$

$$V = V_{INST} + Z_V + K_V A + C_V(B-V) + K_{V2}A(B-V) + C_{V2}(B-V)^2 + t_V t \tag{13}$$

$$R = R_{INST} + Z_R + K_R A + C_R(V-I) + K_{R2}A(V-I) + C_{R2}(V-I)^2 + t_R t \tag{14}$$

$$I = I_{INST} + Z_I + K_I A + C_I(V-I) + K_{I2}A(V-I) + C_{I2}(V-I)^2 + t_I t \tag{15}$$

Where V_{INST} is the instrumental magnitude, Z_V is the zero point of the optical system used, C_V and C_{V2} are the color correction terms, K_V and K_{V2} are the extinction coefficients, and $t_V t$ models any time dependence present. The minimum number of these coefficients are solved for in order to generate a satisfactory fit Fitzgerald et al. (2021). This error is presented alongside the calculation results.

This study has determined the period of RRab RR Lyrae stars X Ari and RU Scl to be 0.652 days and 0.494 days respectively, which supports previously measured periods from alternate studies. The period of the classical type II Cepheid star OP Pup was found to be 2.597 days, which supports the only-once previously reported claim that OP Pup is indeed a classical Cepheid rather than a RR Lyrae star as previously thought. Light curves taken in Bessel V have been found and presented as well for all three stars studied. The distance estimations of (463 ± 19)pc in V, (667 ± 30)pc in ip, and (8775 ± 483)pc in Z for X Ari do not agree with GAIA's parallax measurement of

(544.722 ± 5.5783)pc. The calculated distances of (780 ± 31)pc in V, (781 ± 37)pc in ip, and (664 ± 48)pc in Z for RU Scl agree with GAIA's parallax measurement of (798.148 ± 20.1942)pc in the V and ip filters, but not in the Z band. The distances found of (450 ± 25)pc in V, (711 ± 25)pc in ip, and (864 ± 28)pc in Z for OP Puppis do not agree with GAIA's parallax measurement of (2509 ± 23)pc. This confirms that the RRL PL relations utilized within this study are not communicative to other types of variable stars with extended periods and also supports the suspected lack of metallicity dependence on T2C periods in the optical and near-IR bands. Using alternative PL equations that have been calibrated for Cepheids, distance calculations yielded (2556.669 ± 26)pc in V from Carroll & Ostlie (1996) and (2398.492 ± 26)pc in B, (2416.8025 ± 26)pc in V, and (3058.27055 ± 26)pc in ip from Sandage et al. (2009) all lie much closer to GAIA's parallax measurement of (2509 ± 23)pc for OP Puppis. The wildly differing Z band results for X Ari can be attributed to lack of quality within the cadenced images received for the star, but even still there is an apparent lack of accuracy in the Z filter for RU Scl as well; indicating a need for a revisit of the calibration of the coefficients for the M_Z PL relationship. The M_V and M_{ip} RR Lyrae Period-Luminosity relationships demonstrated an average difference of 3.8% and 2.2% compared against GAIA DR3 parallax measurements for X Ari and RU Scl respectively, indicating that there is still work to be done calibrating the coefficients of the PL equations for maximum precision, however currently the equations are accurate enough for analysis within the visual and near-visual wavelength bands on relatively local RR Lyrae variable stars for comparison against geometric parallax measurements of missions such as GAIA.

REFERENCES

Beers, T. C., Chiba, M., Yoshii, Y., et al. 2000, AJ, 119, 2866, doi: 10.1086/301410

Bond, H. E., Perry, C. L., & Bidelman, W. P. 1971, PASP, 83, 643, doi: 10.1086/129191

Bono, G., Braga, V. F., Crestani, J., et al. 2020, ApJL, 896, L15, doi: 10.3847/2041-8213/ab9538

Breuval, L., Riess, A. G., Casertano, S., et al. 2024, Small Magellanic Cloud Cepheids Observed with the Hubble Space Telescope Provide a New Anchor for the SH0ES Distance Ladder. https://arxiv.org/abs/2404.08038

Carrillo, D., Burki, G., Mayor, M., et al. 1995, A&AS, 113, 483

Carroll, B. W., & Ostlie, D. A. 1996, An Introduction to Modern Astrophysics

Catelan, M., Pritzl, B. J., & Smith, H. A. 2004, The Astrophysical Journal Supplement Series, 154, 633–649, doi: 10.1086/422916

Chadid, M., Sneden, C., & Preston, G. W. 2017, ApJ, 835, 187, doi: 10.3847/1538-4357/835/2/187

Clem, J. L., & Landolt, A. U. 2013, AJ, 146, 88, doi: 10.1088/0004-6256/146/4/88

—. 2016, AJ, 152, 91, doi: 10.3847/0004-6256/152/4/91

Clementini, G., Eyer, L., Ripepi, V., et al. 2017, Astronomy amp; Astrophysics, 605, A79, doi: 10.1051/0004-6361/201629925

Clementini, G., Ripepi, V., Molinaro, R., et al. 2019, Astronomy amp; Astrophysics, 622, A60, doi: 10.1051/0004-6361/201833374

Collins, K. A., Kielkopf, J. F., Stassun, K. G., & Hessman, F. V. 2017, The Astronomical Journal, 153, 77, doi: 10.3847/1538-3881/153/2/77

Crestani, J., Braga, V. F., Fabrizio, M., et al. 2021, ApJ, 914, 10, doi: 10.3847/1538-4357/abfa23

Cáceres, C., & Catelan, M. 2008, The Astrophysical Journal Supplement Series, 179, 242–248, doi: 10.1086/591231

Dambis, A. K., Berdnikov, L. N., Kniazev, A. Y., et al. 2013, MNRAS, 435, 3206, doi: 10.1093/mnras/stt1514

Duflot, M., Figon, P., & Meyssonnier, N. 1995, A&AS, 114, 269

DÃ©kÃ¡ny, I., KovÃ¡cs, G., Jurcsik, J., et al. 2008, Monthly Notices of the Royal Astronomical Society, 386, 521–530, doi: 10.1111/j.1365-2966.2008.13060.x

Feast, M. W., Laney, C. D., Kinman, T. D., van Leeuwen, F., & Whitelock, P. A. 2008, MNRAS, 386, 2115, doi: 10.1111/j.1365-2966.2008.13181.x

Fernley, J. A., Lynas-Gray, A. E., Skillen, I., et al. 1989, MNRAS, 236, 447, doi: 10.1093/mnras/236.3.447

Fitzgerald, M. T., Gomez, E., Salimpour, S., & Wibowo, R. W. 2021, The Journal of Open Source Software, 7. http://dx.doi.org/10.3847/1538-3881/153/2/77

Frolov, M. S. 1976, Information Bulletin on Variable Stars, 1097, 1

Gaia Collaboration. 2022, VizieR Online Data Catalog: Gaia DR3 Part 4. Variability (Gaia Collaboration, 2022), VizieR On-line Data Catalog: I/358. Originally published in: Astron. Astrophys., in prep. (2022)

Gavrilchenko, T., Klein, C. R., Bloom, J. S., & Richards, J. W. 2014, Monthly Notices of the Royal Astronomical Society, 441, 715–725, doi: 10.1093/mnras/stu606

Haschke, R., Grebel, E. K., Frebel, A., et al. 2012, AJ, 144, 88, doi: 10.1088/0004-6256/144/3/88

Hoffman, D. I., Harrison, T. E., & McNamara, B. J. 2009, AJ, 138, 466, doi: 10.1088/0004-6256/138/2/466

Jayasinghe, T., Stanek, K. Z., Kochanek, C. S., et al. 2019, Monthly Notices of the Royal Astronomical Society, doi: 10.1093/mnras/stz844

Joy, A. H. 1938, PASP, 50, 302, doi: 10.1086/124968

Klein, C. R., Richards, J. W., Butler, N. R., & Bloom, J. S. 2011, ApJ, 738, 185, doi: 10.1088/0004-637X/738/2/185

—. 2014, MNRAS, 440, L96, doi: 10.1093/mnrasl/slu031

Kolenberg, K., & Bagnulo, S. 2009, A&A, 498, 543, doi: 10.1051/0004-6361/200811591

Kukarkin, B. V., Kholopov, P. N., Fedorovich, V. P., et al. 1977, Information Bulletin on Variable Stars, 1248, 1

Kunder, A., Kordopatis, G., Steinmetz, M., et al. 2017, AJ, 153, 75, doi: 10.3847/1538-3881/153/2/75

Lafler, J., & Kinman, T. D. 1965, ApJS, 11, 216, doi: 10.1086/190116

Le Borgne, J. F., Paschke, A., Vandenbroere, J., et al. 2007, Astronomy amp; Astrophysics, 476, 307–316, doi: 10.1051/0004-6361:20077957

Li, L. J., Qian, S. B., & Zhu, L. Y. 2018, ApJ, 863, 151, doi: 10.3847/1538-4357/aad32f

Limberg, G., Rossi, S., Beers, T. C., et al. 2021, ApJ, 907, 10, doi: 10.3847/1538-4357/abcb87

Lindegren, L., Klioner, S. A., Hernández, J., et al. 2021, Astronomy amp; Astrophysics, 649, A2, doi: 10.1051/0004-6361/202039709

Maintz, G. 2005, Astronomy amp; Astrophysics, 442, 381–384, doi: 10.1051/0004-6361:20053230

Manduca, A., Bell, R. A., Barnes, T. G., I., Moffett, T. J., & Evans, D. S. 1981, ApJ, 250, 312, doi: 10.1086/159377

Marconi, M., Coppola, G., Bono, G., et al. 2015, ApJ, 808, 50, doi: 10.1088/0004-637X/808/1/50

Muraveva, T., Delgado, H. E., Clementini, G., Sarro, L. M., & Garofalo, A. 2018, MNRAS, 481, 1195, doi: 10.1093/mnras/sty2241

Nagarajan, P., Weisz, D. R., & El-Badry, K. 2022, The Astrophysical Journal, 932, 19, doi: 10.3847/1538-4357/ac69e6

Neeley, J. R., Marengo, M., Bono, G., et al. 2017, ApJ, 841, 84, doi: 10.3847/1538-4357/aa713d

Nemec, J. M., Cohen, J. G., Ripepi, V., et al. 2013, ApJ, 773, 181, doi: 10.1088/0004-637X/773/2/181

Oke, J. B. 1966, ApJ, 145, 468, doi: 10.1086/148787

Padmanabhan, N., Schlegel, D. J., Finkbeiner, D. P., et al. 2008, ApJ, 674, 1217, doi: 10.1086/524677

Ripepi, V., Molinaro, R., Musella, I., et al. 2019, Astronomy amp; Astrophysics, 625, A14, doi: 10.1051/0004-6361/201834506

Ripepi, V., Catanzaro, G., Molinaro, R., et al. 2021, MNRAS, 508, 4047, doi: 10.1093/mnras/stab2460

Samolyk, G. 2010, JAAVSO, 38, 12

Sandage, A., Tammann, G. A., & Reindl, B. 2009, A&A, 493, 471, doi: 10.1051/0004-6361:200810550

Sesar, B., Fouesneau, M., Price-Whelan, A. M., et al. 2017, ApJ, 838, 107, doi: 10.3847/1538-4357/aa643b

Skarka, M. 2014a, A&A, 562, A90, doi: 10.1051/0004-6361/201322491

—. 2014b, MNRAS, 445, 1584, doi: 10.1093/mnras/stu1815

Skowron, D. M., Skowron, J., Mróz, P., et al. 2019, Science, 365, 478–482, doi: 10.1126/science.aau3181

Steinmetz, M., Guiglion, G., McMillan, P. J., et al. 2020, AJ, 160, 83, doi: 10.3847/1538-3881/ab9ab8

Stellingwerf, R. F., Gautschy, A., & Dickens, R. J. 1987, ApJL, 313, L75, doi: 10.1086/184834

Williams, D. B. 1996, JAAVSO, 24, 86

Wilson, R. E. 1953, Carnegie Institute Washington D.C. Publication, 0

Zgirski, B., Pietrzyński, G., Górski, M., et al. 2023, ApJ, 951, 114, doi: 10.3847/1538-4357/acd63a